Rare Metal Materials and Engineering
Volume 51, Issue 2, February 2022
Available online at www.rmme.ac.cn

Science Press

Cite this article as: He Longchao, Jing Lei, Yu Sen, et al. Effect of Second Phase on Corrosion Behavior of WE43 Alloy[J]. Rare Metal Materials and Engineering, 2022, 51(02): 484-490.

ARTICLE

Effect of Second Phase on Corrosion Behavior of WE43 Alloy

He Longchao[1,2], Jing Lei[2], Yu Sen[2], Yu Zhentao[3]

[1] College of Materials Science and Engineering, Northeastern University, Shenyang 110819, China; [2] Northwest Institute for Nonferrous Metal Research, Xi'an 710016, China; [3] College of Chemistry and Materials Science, Jinan University, Guangzhou 510632, China

Abstract: Microstructure analysis, EDS analysis, mass loss experiment and electrochemical test were used to detect the corrosion performance of WE43 alloy after solution and solution-aging treatment. The result shows that heat treatment changes the second phase in the matrix to obtain different corrosion properties. The corrosion rate of solution-aging samples immersed for 0 and 6 h is higher than that of solution samples, and lower than that of solution sample immersed for 24 h. It is also found that during the corrosion process of WE43 alloy, the corrosion rate decreases first and then increases. Mathematical model was used to explain the relationship between the second phase and corrosion performance, and the reason why the corrosion rate changes with time.

Key words: WE43 alloy; magnesium; solution treatment; solution-aging treatment; corrosion rate

At present, medical materials can be roughly divided into four types: ceramics, polymers, metals, composites[1]. A 70 kg adult contains about 20~28 g magnesium. Mg and Mg alloys have received extensive attention in the field of degradable materials, since they have similar elastic modulus to bone, thus avoiding "stress shielding" [2, 3]. However, the corrosion rate of magnesium and magnesium alloys in the human body is too fast, and a large amount of Mg^{2+} is produced, which causes an imbalance in the human body environment, leading to increased cytotoxicity and serious impact on its biocompatibility. Scientists mainly focus on high-purity magnesium, alloying and composite materials to reduce the degradation rate of Mg implants in the body and to improve biocompatibility. For ideal biodegradable medical metals, the implant maintains complete mechanical properties within 12 months, and can be completely degraded after 12~24 months. Corrosion products are absorbed by the body or excreted, which requires a degradation rate of <0.02 mm·a^{-1}. The self-corrosion potential of Mg is low (-2.37 V). When galvanic corrosion occurs, Mg acts as the anode of the electrode reaction. The corrosion products ($MgOH_2$) covering the surface of Mg can reduce the corrosion rate to a certain extent. There is a large amount of Cl^- in the human body environment, which reacts with $Mg(OH)_2$ to generate $MgCl_2$[4].

In order to reduce the corrosion rate, the addition of alloy elements to Mg alloy is needed to change the chemistry. Zirconium- and Yttrium-phases have been shown to impact the corrosion rate. The second phase formed by adding alloying elements has a significant impact on the corrosion performance of the alloy. However, there is no consensus on the influence of second phase on the corrosion performance of magnesium, and no unified statement has been formed. For the AZ91 alloy, the precipitation of the $Mg_{17}Al_{12}$ forms a micro-coupling with α-Mg to accelerate its corrosion rate, but when the size of $Mg_{17}Al_{12}$ reaches a certain level, it can also act as a barrier between the substrate and the outside to reduce the corrosion rate[5]. The as-cast Mg-6Zn alloy is treated at a temperature of 360 °C for 6~48 h to control the re-dissolution of the second phase, and the corrosion rate measured by SBF (simulated body fluid) shows that the second phase re-dissolves when the solution treatment is 24 h, and the corrosion rate is increased by 60% compared with that of the cast status[6].

In this study, by measuring the mass loss, electrochemical performance, and microstructure in 3% NaCl solution, the influence of the second phase on the corrosion performance of

Received date: February 16, 2021
Foundation item: National Natural Science Foundation of China (2020ZDLGY1)
Corresponding author: Yu Zhentao, Ph. D., Professor, College of Chemistry and Materials Science, Jinan University, Guangzhou 510632, P. R. China, Tel: 0086-29-86231084, E-mail: yzt@c-nin.com

Copyright © 2022, Northwest Institute for Nonferrous Metal Research. Published by Science Press. All rights reserved.

WE43 alloy was explored and the corrosion performance was explained through mathematical models.

1 Experiment

The WE43 alloy plates used in the experiment were provided by Luoyang Mage Magnesium Company. Before the experiment, the composition of the alloy was detected by induced couple plasma mass spectrometry (ICP-MS). Table 1 shows composition analysis results of WE43 alloy.

Then samples were treated with solution treatment and solution-aging treatment to change the content of the second phase. Solution samples were placed at 500 °C for 12 h, followed by water quenching, namly "solution treatment". Based on the process of solution treatment of samples, solution-aging samples were heated for 24 h at 300 °C, followed by water quenching, namly "solution-aging treatment". Then WE43 was cut into 10 mm×10 mm×4 mm specimens by wire cutting. In order to remove impurities on the surface, specimens were cleaned in warm water with metal cleaning agent for 20 min, then ground to 2000# grit by metallographic sandpaper. The phase of the sample was detected by X-ray diffraction (XRD).

The samples were soaked in 3% NaCl for 7 d, and ratio of sample area to solution volume was 1 cm^2: 20 mL. The corrosion products of sample were removed by 200 $g \cdot L^{-1}$ CrO_3+10 $g \cdot L^{-1}$ $AgNO_3$ for 15 min after the immersion test. Rinse the corrosion products of the sample with deionized water and measure mass loss.

The open circuit potential and polarization curve were measured by electrochemical equipment. Electrochemical measuring equipment adopted traditional three-electrode mode, with the sample as working electrode, platinum (Pt) as counter electrode, and saturated calomel electrode as reference electrode. First, the open circuit potential was performed from -2.5 V to -0.5 V at 5 mV/s after immersion for 0, 6 and 24 h. And repeat all electrochemical tests at least 3 times. Corrosion current density and corrosion potential were obtained by line Tafel extrapolation. JSM-6460 SEM equipped with energy spectrum analysis (EDS analysis) was use to analyze the microstructure before and after corrosion.

Table 1 Chemical composition of WE43 alloy (wt%)

Y	Nd	Zr	Mg
3.99	3.81	0.53	Bal.

2 Results and Discussion

2.1 Microstructure of WE43 alloy after heat treatment

Fig. 1 shows the micromorphology of samples before immersion. Fig. 1a shows the SEM morphology of the base metal, and a large number of band-like second phases can be seen. After solution-treatment, the second phases dissolve and the degree of uniformity of the microstructure is improved (Fig. 1b), but the second phases can be observed in the matrix, and this common phenomenon can be attributed to the Gibbs-Thompson effect. Thompson effect believed that the solubility of alloying elements in the matrix depends on the curvature of the second phase in the matrix[7]. Fig. 1c shows the precipitation of the second phases after solution-aging treatment at 300 °C. Fig. 1d shows the microstructure after solution treatment, and it can be seen that there are two second phases with completely different sizes, the smaller second phase is Y-rich and the larger particle is Zr-rich. The result of the EDS analysis on the second phase is shown in

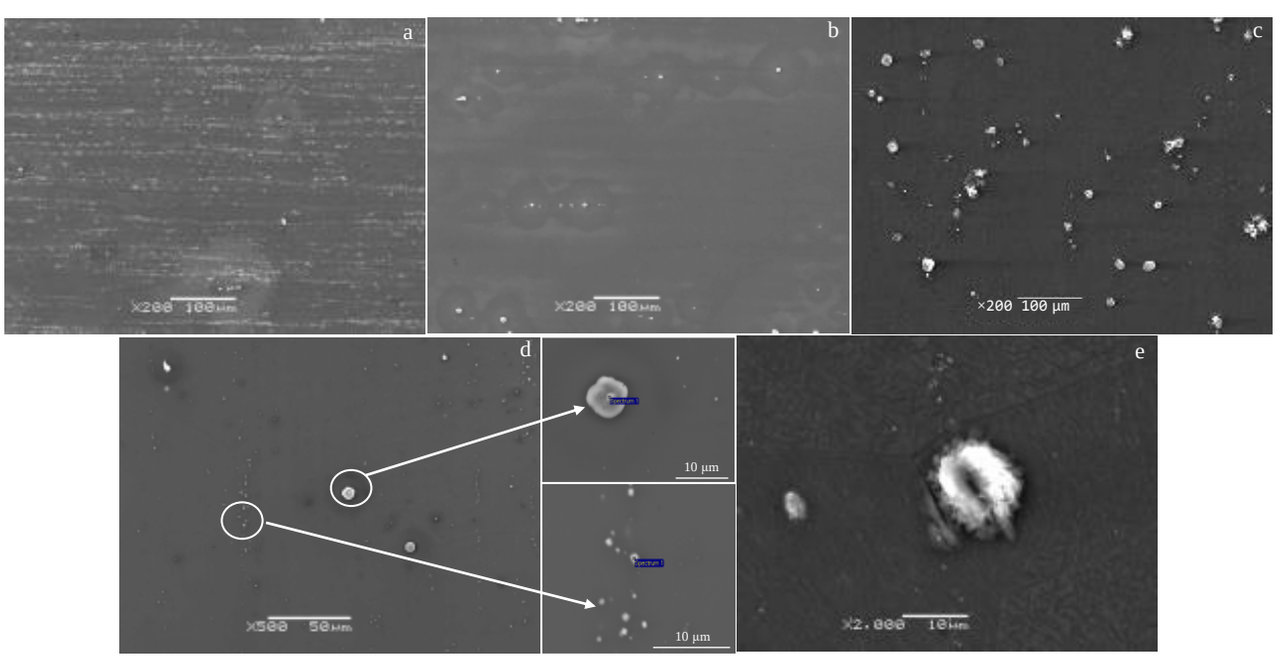

Fig. 1 SEM images of samples before immersion: (a) WE43, (b, d) solution treated, and (c) solution-aging treated, and (e) second phases precipitated in matrix

Fig. 1d, Table 2 and Table 3. Wang[8] reported that Zr-rich and Y-rich have higher solution temperature, which cannot dissolve in Mg matrix at 500 °C. Fig. 1e shows a large number of fine second phases precipitated in the matrix. It is believed that the second phases in magnesium alloys are Zr-rich and Y-rich precipitates, which have the greatest impact on corrosion performance[9,10]. Fig. 2 shows the XRD patterns of solution treated and solution-aging treated sample.

2.2 Corrosion performance evaluation

The results of the mass loss experiment can more intuitively reflect the corrosion performance of the material. The mass loss calculation formula is as follows:

Table 2 EDS analysis of Zr-phase (larger particle) in Fig.1d

Element	wt%	at%
Mg	1.58	5.68
Zr	98.42	94.32

Table 3 EDS analysis of Y-phase (smaller second phase) in Fig.1d

Element	wt%	at%
Mg	27.74	60.13
Y	60.04	35.59
Nd	6.16	2.25
Gd	6.05	2.03

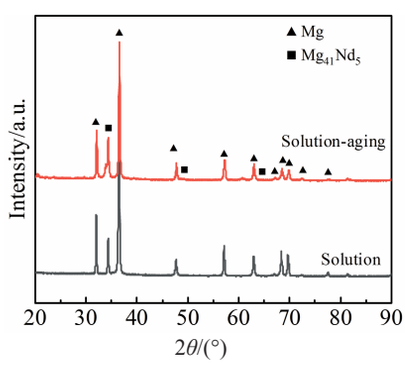

Fig.2 XRD patterns of solution treated and solution-aging treated samples

$$v = \frac{\Delta m}{St} \quad (1)$$

where v is corrosion rate, Δm is mass change before and after corrosion, S is the area of the sample exposed to the solution, t is immersion time. Fig. 3 shows the average corrosion rate (Δm) in 7 d. It can be seen that the corrosion performance after solution treatment is lower than that of solution-aging treatment.

Fig. 4 shows the open circuit potential of the test sample immersed in 3% NaCl solution for 600 s. Table 4 show the corrosion current density and corrosion potential of the sample immersed in 3% NaCl solution for 0, 6 and 24 h, and it can be seen that the corrosion rate of WE43 alloy first decreases and then increases. Fig. 5 shows the polarization curve of the sample immersed in 3% NaCl solution for 0, 6 and 24 h. When soaking for 0 and 6 h, the corrosion resistance of solution treated alloy is better than that of solution-aging treated alloy. In contrast, the corrosion resistance of solution-aging treated alloy is better when soaking for 24 h. It can be seen from Fig. 5b that when the immersion time is 6 h, the maximum corrosion current of the sample is three times larger than that of 0 and 24 h.

2.3 Characterization of micromorphology after corrosion

Fig. 6 shows the morphologies of WE43 before and after removing corrosion products after 7 d of immersion. A large number of corrosion products fall off from the surface (Fig.6a). It can be seen that there are many pits on the surface after removing the corrosion products, and the solution treatment samples have serious pitting corrosion (Fig. 6b).

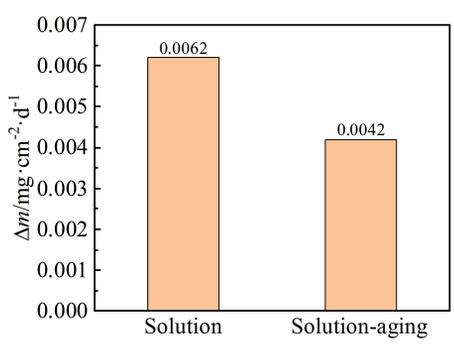

Fig.3 Average corrosion rate within 7 d of immersion

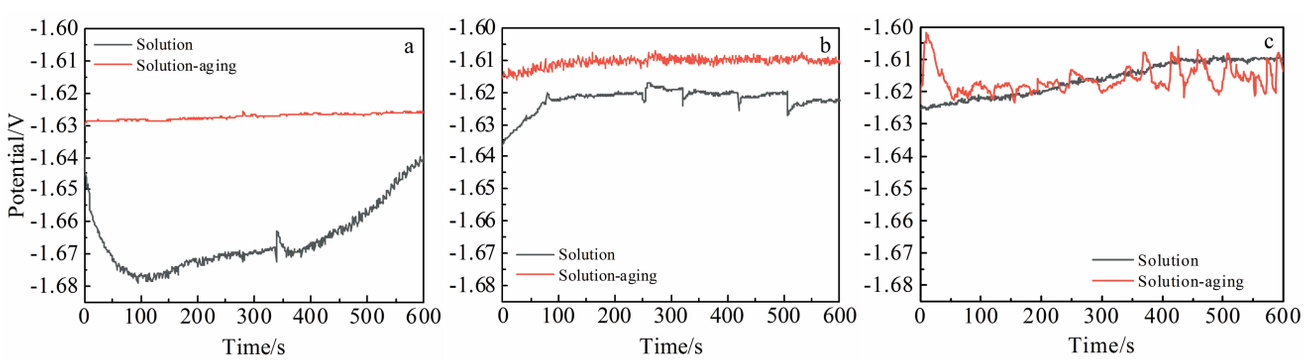

Fig.4 Open circuit potential of the test samples immersed in 3% NaCl solution for 600 s: (a) 0 h, (b) 6 h, and (c) 24 h

Table 4 Corrosion current density and corrosion potential of the samples immersed in 3% NaCl solution

Sample	Immersion time/h	Polarization potential/V	Corrosion current density/μA·cm^{-2}
Solution	0	-1.7	1883.33
	6	-1.39	50.06
	24	-1.507	1333.33
Solution-aging	0	-1.68	2130
	6	-1.341	79.2
	24	-1.34	189.5

Fig. 6c shows that there is a large amount of dome after solution-aging treatment. Reference reported a detailed explanation of the formation of domes. Compared with the solution treatment, the corrosion products of the solution-aging treated samples have a better protective effect on Mg.

Fig. 7a shows micromorphology of solution-treated samples after removing corrosion products. It can be found that the corrosion performance of the area closer to the second phases is superior to that farther away from second phases. Fig. 7b shows solution-aging treated morphology. There are a lot of cracks on the surface, which are caused by the destruction of the corrosion film by H_2. It can be attributed to the presence of a large amount of precipitated phases as the cathode in the solution-aging sample, which lead to a fine dispersion of the generated H_2.

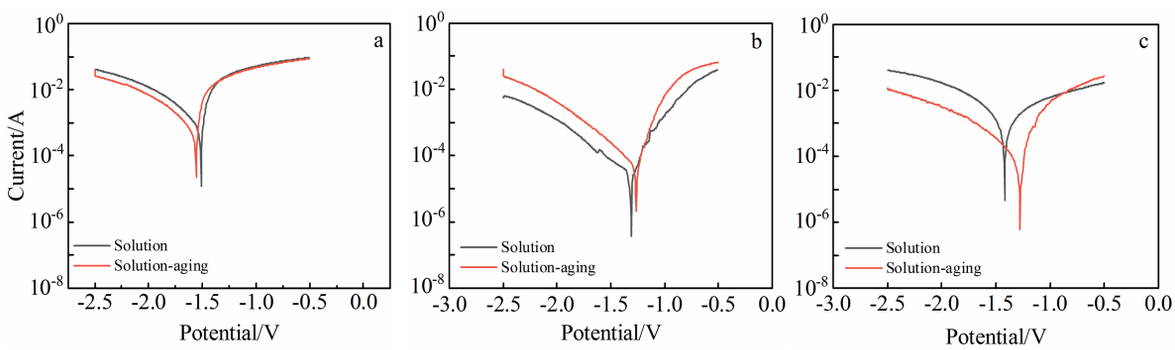

Fig.5 Polarization curves of samples immersed in 3% NaCl solution for 0 h (a), 6 h (b) and 24 h (c)

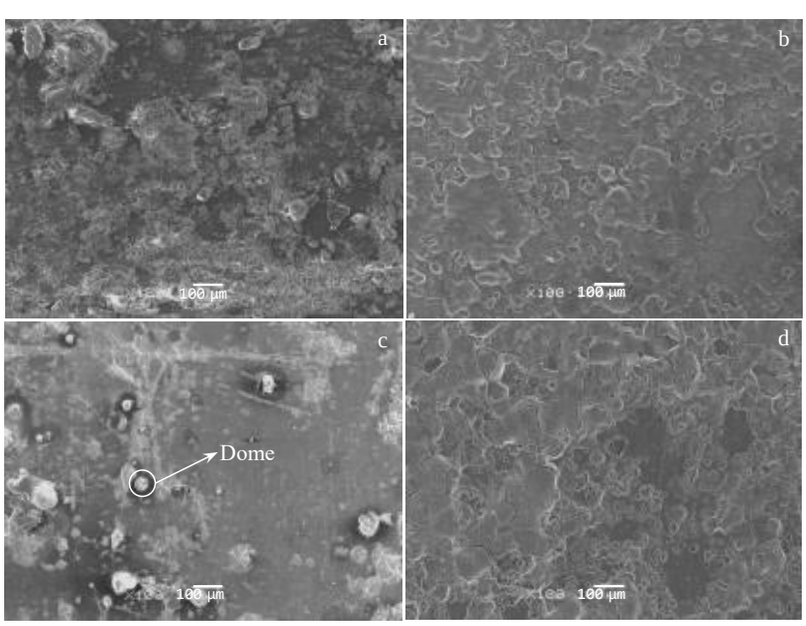

Fig.6 Corrosion morphologies of WE43 alloys with (a, c) and without (b, d) corrosion products after 7 d of immersion: (a, b) solution treated and (c, d) solution-aging treated

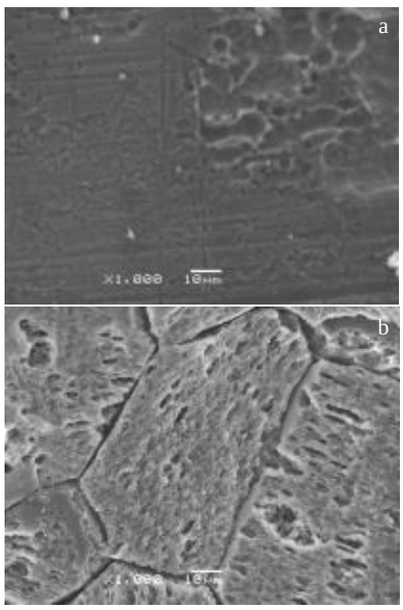

Fig.7 Corrosion morphologies of WE43 alloys after 7 d of immersion: (a) solution treatment with pit and (b) solution-aging treatment with crack

2.4 Discussion

Immersion test is the most direct way to compare corrosion performance[11]. Through mass loss experiments, researchers found that Cl^- and pH in NaCl solution affect the degradation rate of Mg and Mg alloy. In the traditional sense, the content of the second phases in the matrix increases after solution-aging treatment, resulting in an increase in the number of micro galvanic couples and aggravating Mg corrosion. However, in this experiment, the corrosion degradation rate of solution-aging treated samples is higher than that of solution-treated samples through the immersion experiment.

The corrosion rates of solution-aging treated samples are higher than those of the solution treated for 0 and 6 h. When the immersion time is 0 and 6 h, corrosion rate of solution-aging treated samples is higher compared with that of solution treated samples. Table 4 obtained by line Tafel extrapolation shows the same results as above. The reason is follows. There are a large number of micro galvanic couples in the solution-aging treated samples in the early stage of corrosion, which lead to higher corrosion rate compared to solution-treatment samples. According to the Mg corrosion mechanism, hydrogen is mainly generated at the cathode, and the presence of a large number of small second phases produces more H_2 sites, which destroys the corrosion layer on the surface (Fig. 7c). However, Moon[12] reported that H_2 accumulates in the cathode area on the surface of Mg and Mg alloy during the corrosion process, the accumulation of H_2 can hinder the contact between Mg and Cl^- and play a certain protective role. It can be found that the corrosion potential of solution-aging is higher than that of solution, but the corrosion current density is smaller at 0 and 6 h. This indicates that there is a general negative difference effect in the corrosion process of magnesium alloys[13].

2.4.1 Influence of second phases on corrosion rate

Zhang[14] found that in the AZ alloy, the β phase not only forms a micro-couple with the matrix to promote the corrosion rate, but also hinders the contact between H_2O and α-Mg to reduce the corrosion rate. From the experimental results, it is found that the second phases uniformly distributed in the solution-aging treated samples can reduce the corrosion degradation rate. In the corrosion process of WE43 alloy, a dome composed of corrosion products is formed at the second phases[15].

Combined with the results of this experiment, we use Song's mathematical model for the protection of porous films on magnesium surfaces to explore the influence of the second phases on corrosion performance. Ref. [16] used cathode current to characterize the corrosion rate. Corrosion current density is follows:

$$I_c = \theta I_{co} e^{\frac{-(E-E_{ce})}{b_{co}}} + (1-\theta) I_{cp} e^{\frac{-(E-E_{ce})}{b_{cp}}} \quad (2)$$

where θ ($0<\theta<1$) is the ratio of the area that is not occupied by corrosion products to the total area of the magnesium electrode, I_{co} is current density of Mg in product-free area, b_{co} is slope of the Tafel curve without corrosion product covering Mg surface, E_{ce} is equilibrium potential without corrosion product coverage; I_{cp} is current density of Mg under corrosion products, b_{cp} is slope of the Tafel curve with corrosion products covering the surface of Mg, and E is electrode potential. Compared with areas not covered by corrosion products, it is difficult to corrode areas covered by corrosion products, so $b_{cp} \rightarrow +\infty$.

The following formula can be obtained:

$$I_c = \theta I_{co} e^{\frac{-(E-E_{ce})}{b_{co}}} \quad (3)$$

Based on Song's research, the trend of corrosion rate is follows:

$$\frac{dI_c}{dt} = \theta I_{co} e^{\frac{-(E-E_{ce})}{b_{co}}} \left(\frac{d\theta}{dt} - \frac{\theta}{b_{co}} \frac{dE}{dt} \right) \quad (4)$$

It is assumed that the potential does not change in each period. It can be simplified to

$$\frac{dI_c}{dt} = I_{co} e^{\frac{-(E-E_{ce})}{b_{co}}} \frac{d\theta}{dt} \quad (5)$$

We use Eq. (5) to explain the effect of second phases on corrosion rate and the change of corrosion rate during the corrosion process. Due to the presence of a large number of micro-couples in solution-aging, the corrosion film is produced at a faster rate, and θ of solution treatment sample is higher. Thus, the relative values of θ agree with the relationship:

$$\theta_{\text{solution-aging}} < \theta_{\text{solution}} \quad (6)$$

The cathode reactions exhibit similar behavior, so the slopes of Tafel curve of solution and solution-aging are estimated to approximately equal to each other. Consequently,

$$b_{\text{co, solution-aging}} \approx b_{\text{co, solution}} \quad (7)$$

The difference between $E_{\text{ce, solution-aging}}$ and $E_{\text{ce, solution}}$ is neglected. E_{solution} is more negative than $E_{\text{solution-aging}}$ compared with the free corrosion potential (Fig. 5). Then,

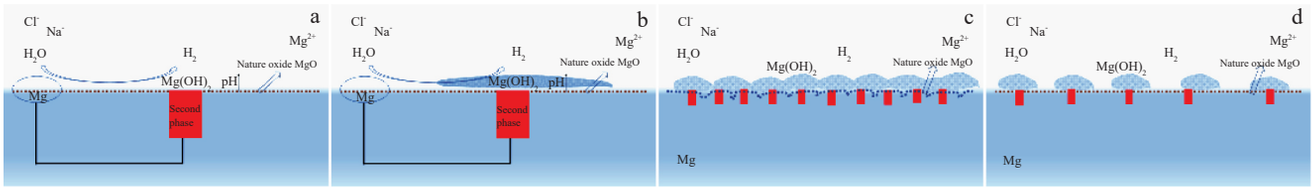

Fig.8 Corrosion mechanism of WE43 alloy in NaCl: (a, b) micro galvanic corrosion, (c) corrosion films of solution treated samples, and (d) corrosion films of solution-aging treated samples

$$e^{\frac{-(E-E_{ce})}{b_{co}}}_{\text{solution - aging}} < e^{\frac{-(E-E_{ce})}{b_{co}}}_{\text{solution}} \quad (8)$$

The relationship can be concluded:

$$I_{c,\text{solution-aging}} < I_{c,\text{solution}} \quad (9)$$

Eq. (9) interprets the relationship of corrosion rates ranked as solution-aging＜solution. However, when the immersion time is 0 and 6 h, the actual result of the experimental test is contrary to the calculated result. This can be attributed to the precipitation of a large number of small second phases at the beginning of the reaction, which form a large number of micro-couples with Mg. The cathodes are finely distributed, the generated H_2 has an enhanced ability to damage the corrosion film, and there is a negative difference effect in magnesium alloys.

We can find that the corrosion rate first increases and then decreases during the corrosion process of Mg (Table 4). According to the experimental results, the solution and solution-aging treated samples are explained by Eq.(5). As the immersion time is 0~6 h, the cathodes generate corrosion product $Mg(OH)_2$, and the area of Mg exposed to NaCl solution decreases. Thus,

$$\frac{d\theta}{dt} < 0 \quad (10)$$

Substituting Eq. (10) into Eq. (5), the conclusion can be drawn:

$$\frac{dI_c}{dt} < 0 \quad (11)$$

When immersion time is 6~24 h, Cl^- destroys $Mg(OH)_2$ and loses its protective effect on Mg, and the contact area of Mg with the NaCl solution increases,

$$\frac{d\theta}{dt} > 0 \quad (12)$$

Then,

$$\frac{dI_c}{dt} > 0 \quad (13)$$

Eq. (11) and Eq. (13) explain why the corrosion current density first increases and then decreases.

2.4.2 Corrosion mechanism

Ref.[17] reported that the oxide film of WE43 alloy has two layers during the corrosion process, i. e. the inner layer of MgO and the outer layer of $Mg(OH)_2$, and the two films are porous. After solution treatment, the content of the second phases is greatly reduced, but the Zr- and Y-phases with high melting point still exist in the matrix and form a micro-couple with Mg (Fig.1b). Sitzmann[18] attributed the local corrosion to the micro galvanic couple formed by the difference between the boundaries and the grain composition of the solution treated samples. Regarding the local corrosion problem, it is not clear whether it is the influence of the second phase or the influence of internal composition of the grains.

It can be seen that after solution-aging treatment, a large number of fine second phases are precipitated in the grains (Fig. 1c). Although the network structure is not formed, the space (50~200 nm) of second phase is fine to interact with corrosion products, and corrosion products can cover the Mg matrix to the greatest extent, so as to achieve the purpose of reducing the corrosion rate.

Fig. 8 shows the corrosion mechanism of solution-treated and solution-aging treated samples in 3% NaCl solution. There are second phases in all samples treated by solution and solution aging (Fig. 1b and 1c). Therefore, they all have a closed loop formed by a micro-electric couple. The second phases as the cathode form a closed circuit with Mg, and generate hydrogen and magnesium hydroxide (Fig.8a). Fig.8b shows that the corrosion products produced by the cathode accumulate on the cathode, which causes the pH to rise, and then the corrosion rate of Mg under the corrosion product coverage decreases. Fig. 8c shows that corrosion products generated by the second phases of the solution-treated sample cannot be connected to each other, and there is Mg in the area that is not covered by the corrosion products. Pitting corrosion increases the area of Mg not covered by corrosion products, and the corrosion rate increases. Compared with the solution treated samples, it can be found that the second phase distance of the solution-aging treated samples is reduced, and the area not covered by corrosion products is reduced. Large area coverage of $Mg(OH)_2$ can not only reduce the corrosion rate by increasing the pH, but also reduce the potential difference between Mg and second-phase covered by corrosion products (Fig.8d).

3 Conclusions

1) In the early stage of immersion, the corrosion rate of solution-aging treated WE43 alloy samples is greater than that of solution treated samples due to the existence of the micro-couple and the negative difference effect.

2) After immersion for a period of time, the corrosion rate of solution-aging treated samples is less than that of solution treated samples. The second phases in the solution sample can reduce the corrosion rate in the surrounding area, the corrosion in the area farther from the second phase is more serious, and the solution treated samples have local corrosion.

The second phases precipitate from the solution-aging sample, and the formed corrosion film can cover Mg more completely. The corrosion film improves the corrosion performance by affecting the local pH and reducing the potential difference.

3) The corrosion rate of solution-aging and solution treated samples first decreases and then increases. This is because the corrosion products generated in the initial stage inhibit the corrosion of magnesium alloys. After a period of time, Cl^- destroys $Mg(OH)_2$, and the corrosion layer loses its protective effect, resulting in an increase in the corrosion rate.

References

1 Tahmasebifar A, Kayhan S M, Evis Z *et al. Journal of Alloys & Compounds*[J], 2016, 687: 906

2 Liu Yuxiang. *Rare Metal Materials and Engineering*[J], 2021, 50 (1): 361

3 Hofstetter J, Martinelli E, Weinberg A M *et al. Corrosion Science* [J], 2015, 91: 29

4 Yang J, Koons G L, Cheng G *et al. Biomedical Materials*[J], 2018, 13(2): 22 001

5 Song G L, Atrens A, John D S *et al. Corrosion Science*[J], 1997, 39(10): 1981

6 Shahri S M G, Idris M H, Jafari H *et al. Transactions of Nonferrous Metals Society of China*[J], 2015, 5: 17

7 Perez M. *Scripta Materialia*[J], 2005, 52: 709

8 Wang X, Zhang P, Dong L H *et al. Materials & Design*[J], 2014, 54: 995

9 Davenport A J, Padovani C, Connolly B J *et al. Electrochemical and Solid-State Letters*[J], 2007, 10(2): 5

10 Gandel D S, Easton M A, Gibson M A *et al. Corrosion Science* [J], 2014, 81: 27

11 Kirkland N T, Birbilis N, Staiger M P. *Acta Biomaterialia*[J], 2012, 8: 925

12 Moon S, Yang C, Pyun S I. *Journal of Solid State Electrochemistry*[J], 2015, 19: 3491

13 Liu L J, Schlesinger M. *Corrosion Science*[J], 2009, 51(8): 1733

14 Zhang W B. *Corrosion Science*[J], 1998, 40(10): 17

15 Chu P, Marquis E A. *Corrosion Science*[J], 2015, 101: 94

16 Li J, Jiang Q, Sun H *et al. Corrosion Science*[J], 2016, 111: 288

17 Taheri M, Danaie M, Kish J R. *Journal of the Electrochemical Society*[J], 2013, 161(3): 89

18 Sitzmann E, Marquis E A. *Philosophical Magazine Letters*[J], 2015, 95(1): 7

WE43合金中第二相对腐蚀降解性能的影响

贺龙朝[1,2]，荆　磊[2]，余　森[2]，于振涛[3]

(1. 东北大学 材料科学与工程学院，辽宁 沈阳 110819)

(2. 西北有色金属研究院，陕西 西安 710016)

(3. 暨南大学 化学与材料学院，广东 广州 510632)

摘　要：采用显微组织观察、EDS分析、失重实验和电化学测试研究了固溶和固溶-时效WE43合金的腐蚀性能。结果表明，通过热处理改变基体中第二相，可得到不同腐蚀性能，固溶-时效试样经0和6 h浸泡后的腐蚀速率高于固溶处理试样的腐蚀速率，然而在浸泡24 h后腐蚀速率低于固溶处理试样。镁合金在腐蚀过程中，腐蚀速率先减小后增大。通过建立数学模型解释第二相对腐蚀性能的影响，以及腐蚀速率随时间改变的原因。

关键词：WE43合金；镁合金；固溶处理；固溶-时效处理；腐蚀速率

作者简介：贺龙朝，男，1995年生，硕士，西北有色金属研究院，陕西 西安 710016，电话：029-86231084，E-mail：helongchao1995@163.com